Water-Soluble Thin Film Transistors and Circuits Based on Amorphous Indium−Gallium−Zinc Oxide

Sung Hun Jin,*,†,¶ Seung-Kyun Kang,⊥,¶ In-Tak Cho,§,¶ Sang Youn Han,⊥,# Ha Uk Chung,⊥ Dong Joon Lee,⊥ Jongmin Shin,§ Geun Woo Baek,† Tae-il Kim,‖ Jong-Ho Lee,*,§ and John A. Rogers*,‡

†Department of Electronic Engineering, Incheon National University, Incheon 406-772, Korea

‡Department of Materials Science and Engineering, Chemistry, Mechanical Science and Engineering, Electrical and Computer Engineering, Beckman Institute for Advanced Science and Technology, and Frederick Seitz Materials Research Laboratory, University of Illinois at Urbana−Champaign, Urbana, Illinois 61801, United States

⊥Department of Materials Science and Engineering and Frederick Seitz Materials Research Laboratory, University of Illinois at Urbana−Champaign, Urbana, Illinois 61801, United States
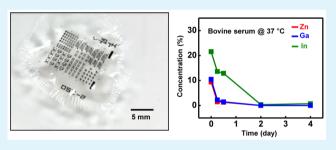
§Department of Electrical Engineering, Seoul National University, Seoul 151-600, Korea

‖Center for Neuroscience Imaging Research (CNIR), Institute of Basic Science (IBS), School of Chemical Engineering, Sungkyunkwan University (SKKU), Suwon, Gyeonggi-do 440-746, Korea

#Display R&D Center, Samsung Display Co., Yongin-city, Gyeongki-do 446−711, Korea

S *Supporting Information*

ABSTRACT: This paper presents device designs, circuit demonstrations, and dissolution kinetics for amorphous indium−gallium−zinc oxide (a-IGZO) thin film transistors (TFTs) comprised completely of water-soluble materials, including SiN_x, SiO_x, molybdenum, and poly(vinyl alcohol) (PVA). Collections of these types of physically transient a-IGZO TFTs and 5-stage ring oscillators (ROs), constructed with them, show field effect mobilities ($\sim$10 cm^2/Vs), on/off ratios ($\sim$2 $\times$ 10^6), subthreshold slopes ($\sim$220 mV/dec), Ohmic contact properties, and oscillation frequency of 5.67 kHz at supply voltages of 19 V, all comparable to otherwise similar devices constructed in conventional ways with standard, nontransient materials. Studies of dissolution kinetics for a-IGZO films in deionized water, bovine serum, and phosphate buffer saline solution provide data of relevance for the potential use of these materials and this technology in temporary biomedical implants.

KEYWORDS: *a-IGZO, transient electronics, dissolution, PVA, inverter, ring oscillators*

1. INTRODUCTION

Research in recent years has established amorphous indium−gallium−zinc oxide (a-IGZO) as the semiconductor for a thin film transistor (TFT) technology that offers several attractive properties compared to amorphous silicon (a-Si), including optical transparency, high mobility, low temperature deposition, and operational stability.[1−5] These features lead to considerable commercial interest for applications in active matrix display devices.

Here, we explore this material for use in a different type of electronics whose key characteristic is the ability to dissolve in water, with potential to enable biologically or environmentally degradable devices, or those that can physically disappear or transform on demand.[6−15] In such classes of transient electronics, a-IGZO has the potential to complement other recently reported water-soluble semiconductors, ranging from biopolymers[16−25] to crystalline silicon.[6,9,11−14] Compared to previous, silicon-based approaches to transient elec-

tronics,[6,9,11−14] a-IGZO offers immediate compatibility with high performance, large-area electronic systems, optical transparency, UV photoresponse,[26] and capabilities in reliable gas sensing,[27] which follow from the amorphous, thin film nature of this material and its large bandgap ($\sim$3 eV). Furthermore, existing data suggest that the constituent elements in a-IGZO have some potential for use in biomedical applications. For example, Ga and In are approved as alloys (e.g., Galloy) by the US Food and Drug Administration (FDA) for dental restoring materials.[28,29] Also, living cells exposed to low concentrations of metal oxides (i.e, In_2O_3 (<50 μg/mL),[30] Ga_2O_3 (<20 μg/mL))[31] exhibit survival rates close to 100%. In inhalation studies, phagocytosis and clearance mechanisms[32] eliminate any toxic effects (See Figure S5, Supporting Information, and Table

1). In addition, previous studies suggest that ZnO at concentrations <100 μg/mL are biocompatible, validated by

Table 1. Summary of Estimation for Volume, Mass, Device Area, and Active Area for a-IGZO Films in Electronic Devices

a-IGZO density [g]	volume [cm^3]	mass [g]	mass for total device area [24.5%] [g]	mass for active area [20%] [g]
3.5	3×10^{-6}	1.05×10^{-5}	2.57×10^{-6}	5.15×10^{-7}
Mass for Each Metal Oxide				
metal oxides	Ga_2O_3		In_2O_3	ZnO
% mass ratio	34		51	15
estimated mass for each metal oxide [g]	$<1.76 \times 10^{-7}$		$<2.61 \times 10^{-7}$	$<7.66 \times 10^{-8}$

cell-based assays[33] and that it can be used in water-soluble thin film transistors and mechanical energy harvesters.[7] Results in the following illustrate the use of a-IGZO with conductors (Mo), insulators (SiO$_x$ and SiN$_x$), and substrate materials (poly(vinyl alcohol)) to yield TFTs and ring oscillator circuits that dissolve completely in water.[6−15] Additional studies focus on the chemistry and kinetics associated with hydrolysis of a-IGZO.

2. EXPERIMENTAL SECTION

2.1. a-IGZO TFTs and Circuits on a Si Substrate. The first step of the fabrication involved electron beam (E-beam) evaporation of a layer of Ni (∼300 nm) onto a silicon wafer with a layer of thermal oxide (∼300 nm) on its surface, followed by plasma-enhanced chemical vapor deposition (PECVD) of SiO$_x$ (∼100 nm) at 300 °C. Photolithographic patterning of Mo (∼70 nm, electron beam evaporation) yielded gate electrodes. A bilayer of SiN$_x$ (∼50 nm) and SiO$_x$ (∼50 nm) deposited by PECVD at 300 °C served the gate

insulator. a-IGZO (∼35 nm) was deposited on the SiO$_x$/Ni/SiO$_2$/Si substrate by RF sputtering (Ar ∼5 mTorr, 50 W, 30 min) at room temperature. The sputtering target for a-IGZO has a mole % ratio of Ga$_2$O$_3$/In$_2$O$_3$/ZnO = 1:1:1 (mol %, Dasom RMS.Inc., Korea). Photolithography and wet etching (D.I. water/HCl = 30:1, 5 s) yielded patterns in the a-IGZO to define the active regions of the devices. A final pattern of Mo (∼70 nm) was formed by electron beam evaporation, photolithography, and lift-off in acetone after removal of SiO$_x$/SiN$_x$ by reactive ion etching (RIE; ∼O$_2$/CF$_4$) to create an opening for contacts. An annealing step (∼150 °C, 10 min, air) in a convection oven completed the fabrication.

2.2. Poly(vinyl alcohol) (PVA) Substrate and Transfer Process. Ten wt % PVA (M_w ∼ 31,000, Sigma-Aldrich, USA) was dissolved in D.I. water at 60 °C overnight. The resulting solution of PVA (∼10 wt %) was drop cast in a plastic container and dried in a convection oven (∼80 °C) overnight. Peeling away the PVA film (∼20 μm) and laminating it onto a slide glass coated with poly-(dimethylsiloxane, PDMS) prepared it for receiving transferred devices and circuits. Thermal release tape (Nitto Denko Co., Japan) provided a means for retrieving a-IGZO devices and circuits from the SiO$_x$/Ni/SiO$_2$/Si substrate by immersion in water. Etching in ferric chloride solution (Sigma-Aldrich, USA) eliminated the Ni on the backside of the devices (See Figure S6, Supporting Information). Gently rinsing in D.I. water at room temperaure and drying under a stream of dry nitrogen prepared the structure for transfer.[15,34] This process involved pressing the tape with circuits on its surface against the PVA film (∼20 μm) on slide glass coated with PDMS. Heating on a hot plate at 100 °C allowed release of the tape. Peeling away the PVA completed the process.

2.3. Dissolution Experiments and Characterization of a-IGZO. a-IGZO (∼35 nm thick) was deposited on thermal oxide (∼300 nm thick) on a Si wafer by sputtering (a-IGZO targets; Kurt J. Lesker, USA; purity ∼99.99% or DASOM RMS. Inc., Korea). Square pads (4 μm × 4 μm) of a-IGZO were patterned by photolithography and etching in hydrochloric acid (D.I. water/HCl = 30:1) for atomic force microscope (AFM) measurements. All other forms of characterization were performed on uniform films. The a-IGZO samples were
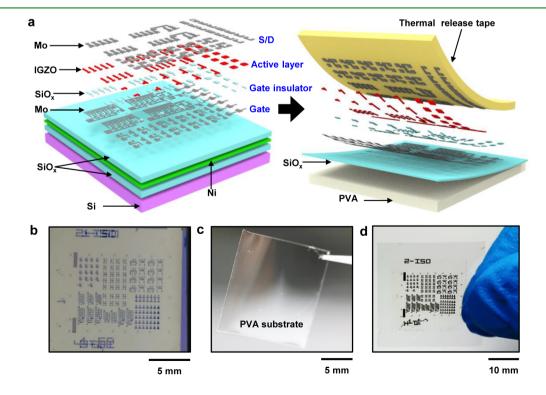

Figure 1. (a) Exploded view schematic illustrations of transient a-IGZO TFTs and circuits first formed on a Si wafer with a sacrificial Ni film (left) and then transferred by a water-assisted process onto a thermal release tape (right). Optical microscope images for (b) fully formed a-IGZO TFTs and circuits on a Si substrate, (c) PVA film as the final device substrate, and (d) devices transferred onto PVA.

immersed in D.I. water, phosphate buffer saline (pH 7.4, Sigma-Aldrich, USA) at 60 °C, or bovine serum (Sigma-Aldrich, USA) at physiological temperature (37 °C). The samples were removed from the solutions, rinsed with D.I. water, cleaned in an ultrasonic cleaner, and measured by AFM (AsylumResearch MFP-3D, USA), X-ray photoelectron spectroscopy (XPS, Axis ULTRA, UK), and X-ray reflectivity (XRR, X'pert MRD system, Netherlands). After such measurements, each of which was completed within a few hours, the samples were returned to the solutions. The solutions were replaced every other day.

2.4. Electrical Characterization of a-IGZO Device and Circuits. Electrical characteristics for a-IGZO TFTs were measured using a semiconductor parameter analyzer (Agilent B1500A). The oscillation frequencies of the 5-stage ring oscillators were measured using an oscilloscope (Tektronix, TDS2012C; input capacitance of 13 pF) connected with an output node of a 2-stage buffer via a 50 Ω coaxial cable terminated at 50 Ω.

3. RESULTS AND DISCUSSION

3.1. Transient a-IGZO Devices and Circuits. Figure 1a presents a schematic diagram of a procedure for fabricating this type of electronics on a Si wafer and then transferring it by water-assisted lift off[15,34] onto a bioresorbable substrate, based on poly(vinyl alcohol) (PVA, $M_w \sim 31,000$), which is known to be biocompatible when prepared in low molecular weight formulations through complete hydrolysis of polyvinyl acetate.[35,36] The process begins with electron beam (E-beam) evaporation of a film of Ni (~300 nm) onto a Si wafer with a layer of thermal oxide (300 nm) on its surface, followed by plasma-enhanced chemical vapor deposition (PECVD) of SiO_x (~100 nm) at 300 °C. E-beam evaporation and photolitho-graphic patterning of Mo (~70 nm) creates gate electrodes. A patterned bilayer of silicon nitride (~50 nm) and silicon oxide (~50 nm) deposited by PECVD at 300 °C serves as a gate dielectric. The semiconductor consists of a layer of a-IGZO formed by RF sputtering at a power of 50 W and a working pressure of 5 mTorr, in Ar at room temperature. Photo-lithography and wet etching (D.I. water/HCl = 30:1) yields patterns in the a-IGZO to define the active regions of the devices. A final pattern of Mo (~70 nm), formed by E-beam evaporation, photolithography, and lift-off in acetone after opening through the SiO_x/SiN_x by reactive ion etching (RIE) with ~O_2/CF_4, forms source/drain electrodes. An annealing step (150 °C for 10 min) completes the process, to yield a system like the one shown in Figure 1b. A set of electrical measurements defines the performance characteristics while on the Si substrate, as a point of comparison against the devices after transfer onto PVA using procedures described next.

Thermal release tape (Nitto Denko Co., Japan) attached on top of the devices enables removal of the entire thin film electronic system upon immersion in water.[15,34] Etching in ferric chloride solution (Sigma-Aldrich, USA) eliminates the Ni on the back side (See Figure S6, Supporting Information).[15] Gently rinsing in water and drying under a stream of dry nitrogen prepares the structure for transfer to a target substrate.[15,34] This process involves pressing the tape, with circuits on its surface, against a PVA film (Figure 1c; ~20 μm thickness, drop cast from solution (~10 wt %) in a plastic container and dried in a convention oven at 80 °C), held onto a PDMS coated glass slide.[15] Heating on a hot plate at 100 °C allows thermal release of the tape. Peeling away the PVA, as shown in Figure 1d, completes the fabrication.

Figure 2a shows a circuit diagram for a 5-stage ring oscillator with a 2-stage buffer, composed of five inverters with a driver
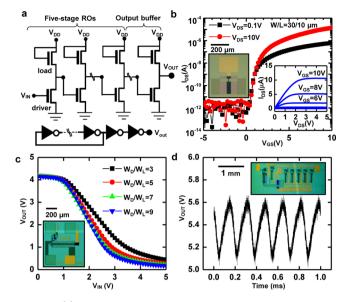

Figure 2. (a) Circuit schematics for an inverter with enhancement load and enhancement driver (ELED) and a 5-stage ring oscillator with a 2-stage output buffer. Electrical characteristics for a-IGZO TFTs and circuits. (b) Transfer characteristics for a-IGZO TFTs with W/L (=30/10 μm). The output characteristics correspond to gate bias values from 0 to 10 V, with 2 V step, for V_{DS} from 0 to 5 V. The inset shows representative a-IGZO TFTs. (c) Voltage transfer character-istics of ELED a-IGZO inverters with ratios of widths of driver (W_D) to load (W_L) transistors between 3 and 9, at a fixed channel length of 10 μm and (d) ring oscillation characteristics for a 5-stage ring oscillator with a 2-stage output buffer, demonstrating a frequency (f_{osc}) of 5.67 kHz at a supply voltage of 19 V. All electrical characteristics were measured before transfer to the PVA substrate.

(W/L = 270/10 μm) and a load (W/L = 30/10 μm) in an enhancement mode. Figure 2b presents representative transfer characteristics for a-IGZO TFTs (W/L = 30/10 μm) in the linear (V_{DS} = 0.1 V) and saturation (V_{DS} = 10 V) regimes, respectively. An optical micrograph of a device appears in the inset. The linear regime data (V_{DS} = 0.1 V) indicate a threshold voltage (~1.94 V), a subthreshold swing (~220 mV/dec), and an on/off ratio (~2×10^6) that are all within the expectation based on previous reports of conventional (i.e., not water-soluble) n-type a-IGZO TFTs.[2−4] The apparent field-effect mobility for devices with channel lengths (L_{ch}), widths (W_{ch}), and transconductance (g_m) at a low drain voltage (V_{DS} = 0.1 V) is determined by $\mu_{FE} = L_{ch} g_m (W_{ch} C_i V_{DS})^{-1}$, where C_i is the gate capacitance per unit area. The mobility computed in this way is ~8−10 cm²/(V s), which is typical of a-IGZO TFTs with similar channel lengths ($L < 10$ μm).[4] Output characteristics appear in the inset of Figure 2b. The data exhibit good saturation behavior and insignificant current crowding at low drain bias ($V_{DS} < 1$), consistent with approximately ohmic behavior at the source/drain contacts. Figure 2c shows the voltage transfer characteristics of inverters with enhancement loads as a function of width ratio ($k \sim (W_D/L_D)/(W_L/L_L)$, where D and L correspond to driver and load) between 3 and 9. As the value of k increases, the peak gains extracted from voltage transfer characteristics (VTC) increase from 1.45 to 2.2, which agrees well with estimated gains for these designs, i.e., peak gain $\sim A_v = (1 + \eta)^{-1} \times ((W/L)_D \times ((W/L)_L)^{-1})^{1/2}$, where η is constant ($\eta > 0$), related with body effects.[37] In addition, five-stage ring oscillators with two-stage buffers, as shown in Figure 2d, exhibit oscillation characteristics at a
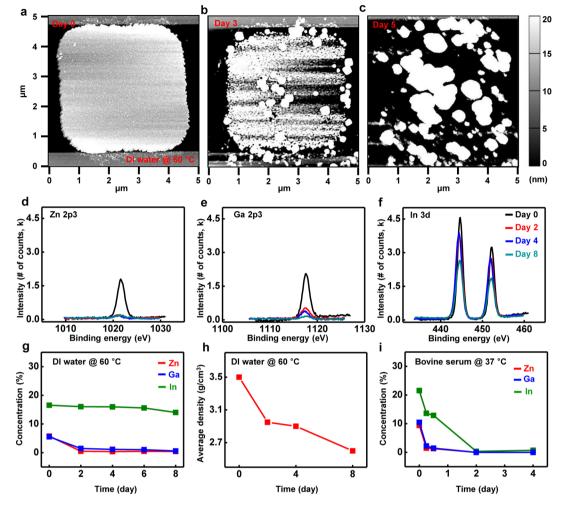
Figure 3. Topographical and chemical evolution of a film of a-IGZO at various stages of dissolution in D.I. water and bovine serum. AFM images of a patterned region of a-IGZO (a) before and after immersion in water at 60 °C for (b) 3 days and (c) 5 days, respectively. Decreases in peak intensities at the characteristic binding energy for (d) Zn, (e) Ga, and (f) In after immersion in the D.I. water at 60 °C, as measured by X-ray photoelectron spectroscopy (XPS) up to 8 days. (g) Evolution of atomic concentration for Zn, Ga, and In at various stages of dissolution in D.I. water at 60 °C. (h) X-ray reflectivity (XRR) analysis for average film density of a-IGZO during immersion in water at 60 °C. (i) Concentration evolution of Zn, Ga, and In for a film of a-IGZO during dissolution in bovine serum at 37 °C.

supply bias of 19 V. Measurements in the inset of Figure 2d, involved an oscilloscope (Tektronix, TDS2012C; input capacitance of 13 pF) connected with an output node of a 2-stage buffer via a 50 Ω coaxial cable terminated at 50 Ω. Generalizing the relationship for an arbitrary odd number of inverters, the oscillation period (T) is given by $T = 2n\tau_\mathrm{p}$, where n is the number of inverters and τ_p is the average propagation delay.[38] The oscillation frequency (f_osc) is 5.67 kHz at a supply voltage of 19 V. By comparison to measurements before transfer, all of these properties are largely unchanged.

3.2. Dissolution Behaviors for a-IGZO Thin Films. The water-soluble nature of these devices represent their key defining attribute. The dissolution properties of the metals, dielectrics, and substrate materials are well-known.[6,8,10,15] Figure 3 summarizes the topographical and chemical evolution of films of a-IGZO associated with dissolution in D.I. water at the temperature of 60 °C (for accelerated testing[10]). Additional studies used bovine serum at physiological temperature (37 °C). Figure 3a shows an atomic force microscope (AFM) image of a patterned film of a-IGZO before immersion in water. The gradual changes in the film appear in a time sequence of AFM images for immersion up to 5 days, in Figure 3b,c. The

dissolution process largely ceases after 5 days, to leave isolated islands of residual material. X-ray intensity of the Zn 2p3, Ga 2p3, and In 3d peaks for various stages of dissolution.

Figure 3d indicates that the Zn 2p3 peak disappears during this process, suggesting consumption by hydrolysis to produce zinc hydroxides[7] ($ZnO + H_2O \leftrightarrow Zn(OH)_2$), which are soluble in aqueous solution. Figure 3e shows that Ga also gradually disappears. Dissolution of Ga oxide by hydrolysis can produce metal hydroxides according to $Ga_2O + 4(OH) \leftrightarrow 2GaO(OH) + H_2O$.[28] Figure 3f shows that the In 3d peaks decrease at a rate slower than those of Zn and Ga. Indium oxide can be removed either by $In_2O_3 + 2H_2O \leftrightarrow 2In\,(OH)_3$ or $In_2O_3 + H_2O \leftrightarrow 2InOOH$.[39] Figure 3g summarizes results of quantitative analysis for Zn, Ga, and In as the dissolution time increases. The data indicate that Zn and Ga disappear within ~2 days, i.e., much more quickly than the In. These observations suggest that the isolated islands that remain after 5 days are predominantly associated with In.

AFM and XPS analysis also suggest that the fast disappearance of Zn and Ga oxides leads to a porous structure as the density of a-IGZO films decreases. Figure 3h shows the average film density measured by X-ray reflectivity (XRR) at
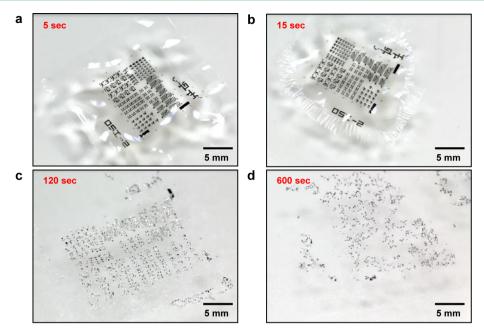
Figure 4. Dissolution of a-IGZO TFTs and circuits on a PVA substrate in D.I. water. A series of optical microscope images collected at various times during dissolution of a-IGZO devices in D.I. water at room temperature for (a) 5 s, (b) 15 s, (c) 120 s, and (d) 600 s. The PVA substrate is fully dissolved after 1800 s, leading to the entire dissociation of the electronic devices in water. Over time, all constituent materials dissolve, although at different rates.

the critical angle (Figure S1, Supporting Information). The sharp decrease in density within 2 days' immersion coincides with removal of Zn and Ga oxides over the same period, observed in Figure 3g. The continuous decrease in density, as shown in Figure 3h, is consistent with continued dissolution of the In oxides, although slowly.

The dissolution kinetics in bovine serum at physiological temperature (37 °C) and in phosphate buffer saline (PBS) at 60 °C, both as representative biofluids, provide data of relevance to the possible use of a-IGZO in temporary implants. In both serum and PBS solution, the Zn and Ga oxides dissolve faster than In oxides, similar to the behavior in D.I. water; however, In oxide also dissolves more quickly than it does in D.I. water (Figures S2−S4, Supporting Information).

Previous reports indicate that reductions in pH improve the solubility of InOH in aqueous solution, consistent with observations here (pH of D.I. water is ∼8.1 and both serum and PBS have pH ∼7.4).[40] In addition, the presence of various ions[41] (i.e, K^+, Na^+, Cl^-, and PO_4^{3-}) in serum and PBS have the potential to accelerate the dissolution, possibly related to the chemistry that underpins the etching of a-IGZO in commonly reported etchants[42] (i.e, KOH, NaOH, $FeCl_3$, and HCl). Because the concentration and type of ions and the pH value can affect the hydrolysis kinetics, additional investigations are needed to fully establish the relevant chemical mechanisms. These results validate that a-IGZO films can be used as a soluble channel material for transient electronics. The images of Figure 4 confirm that the complete system dissolves in D.I. water at room termperature. The PVA substrate (∼20 μm), in the formulation used for this example, largely dissolves within 10 min and disappears entirely in 30 min. This process causes the supported devices to disintegrate. Afterward, each of the remaining constituent materials dissolves at rates defined by their characteristic reactions. The time scales for system survivability can be defined by use of separate encapsulation

and packaging materials or by selection of physical dimensions, film thicknesses, and configurations in the active materials.

4. CONCLUSION

a-IGZO TFTs and circuits built with them offer options in the design and operation of thin film, water-soluble electronics. The electrical data from these transient devices indicate characteristics that are comparable to those of their conventional counterparts. Furthermore, dissolution studies on a-IGZO films in D.I. water and PBS at 60 °C and in bovine serum at 37 °C indicate that oxides of In, Ga, and Zn are soluble through reactions with the corresponding hydroxides, as substantiated by XPS and AFM analysis. Moreover, the demonstration of dissolution of complete a-IGZO circuits beginning with disintegration initiated by elimination of the PVA substrate within 30 min in D.I. water suggests application possibilities in biologically and environmentally resorbable technologies.

■ ASSOCIATED CONTENT

Ⓢ Supporting Information

Change of critical angle of IGZO measured by XRR; intensity of characteristic binding energies corresponding to In, Zn, and Ga after dissolving in bovine serum at 37 °C; atomic concentration of IGZO as a function of time of immersion in phosphate buffer saline at 60 °C; dissolution of IGZO with different initial composition in bovine serum at 37 °C; AFM images for the surface of patterned IGZO film on a thermal oxide/Si substrate and the same sample after dissolution in bovine serum at 37 °C; optical microscope image for a-IGZO FETs and their circuits implemented on carrier substrates with structures of Si/oxide/Ni film before being released in D.I. water; device area estimation from optical images by using Image J software; table for summary of estimation for volume, mass, device area, and active area for a-IGZO films on the implemented substrates; XPS analysis before and after Ni etching during transfer printing process to confirm the residue

of Ni film. This material is available free of charge via the Internet at http://pubs.acs.org.

■ AUTHOR INFORMATION

Corresponding Authors
*E-mail: jrogers@illinois.edu (J.A.R.).
*E-mail: jhl@snu.ac.kr (J.-H.L.).
*E-mail: shjin@inu.ac.kr (S.H.J.).

Author Contributions
¶S.H.J., S.-K.K., and I.-T.C. contributed equally.

Notes
The authors declare no competing financial interest.

■ REFERENCES

(1) Nomura, K.; Ohta, H.; Takagi, A.; Kamiya, T.; Hirano, M.; Hosono, H. Room-Temperature Fabrication of Transparent Flexible Thin-Film Transistors Using Amorphous Oxide Semiconductors. *Nature* **2004**, *432*, 488−492.

(2) Kim, C.; Kang, D.; Song, I.; Park, J.; Lim, H.; Kim, S.; Lee, E.; Chung, R.; Lee, J.; Park, Y. Highly Stable Ga_2O_3-In_2O_3-ZnO TFT for Active-Matrix Organic Light-Emitting Diode Display Application. *Tech. Dig. - Int. Electron Devices Meet.* **2006**, 307−310.

(3) Park, J. S.; Jeong, J. K.; Mo, Y. G.; Kim, H. D.; Kim, S. I. Improvements in the Device Characteristics of Amorphous Indium Gallium Zinc Oxide Thin-Film Transistors by Ar Plasma Treatment. *Appl. Phys. Lett.* **2007**, *90*, 262106-1−262106-3.

(4) Kim, M.; Jeong, J. H.; Lee, H. J.; Ahn, T. K.; Shin, H. S.; Park, J. S.; Jeong, J. K.; Mo, Y. G.; Kim, H. D. High Mobility Bottom Gate InGaZnO Thin Film Transistors with SiO_x Etch Stopper. *Appl. Phys. Lett.* **2007**, *90*, 212114-1−212114-3.

(5) Salvator, G. A.; Münzenrieder, N.; Kinkeldei, T.; Petti, L.; Zysset, C.; Strebel, I.; Büthe, L.; Tröster, G. Wafer-Scale Design of Lightweight and Transparent Electronics that Wraps around Hairs. *Nat. Commun.* **2014**, *5*, 1−8.

(6) Hwang, S.-W.; Tao, H.; Kim, D.-H.; Cheng, H.; Song, J.-K.; Rill, E.; Brenckle, M. A.; Panilaitis, B.; Won, S. M.; Kim, Y.-S.; Song, Y. M.; Yu, K. J.; Ameen, A.; Li, R.; Su, Y.; Yang, M.; Kaplan, D. L.; Zakin, M. R.; Slepian, M. J.; Huang, Y.; Omenetto, F. G.; Rogers, J. A. A Physically Transient Form of Silicon Electronics. *Science* **2012**, *337*, 1640−1644.

(7) Dagdeviren, C.; Hwang, S.-W.; Su, Y.; Kim, S.; Cheng, H.; Gur, O.; Haney, R.; Omenetto, F. G.; Huang, Y.; Rogers, J. A. Transient, Biocompatible Electronics and Energy Harvesters Based on ZnO. *Small* **2013**, *9*, 3398−3404.

(8) Yin, L.; Cheng, H.; Mao, S.; Haasch, R.; Liu, Y.; Xie, X.; Hwang, S.-W.; Jain, H.; Kang, S.-K.; Su, Y.; Li, R.; Huang, Y.; Rogers, J. A. Dissolvable Metals for Transient Electronics. *Adv. Funct. Mater.* **2014**, *24*, 645−658.

(9) Hwang, S.-W.; Park, G.; Cheng, H.; Song, J.-K.; Kang, S.-K.; Yin, L.; Kim, J.-H.; Omenetto, F. G.; Huang, Y.; Lee, K.-M.; Rogers, J. A. 25th Anniversary Article: Materials for High-Performance Biodegradable Semiconductor Devices. *Adv. Mater.* **2014**, *26*, 1992−2000.

(10) Kang, S.-K.; Hwang, S.-W.; Cheng, H.; Yu, S.; Kim, B. H.; Kim, J.-H.; Huang, Y.; Rogers, J. A. Dissolution Behaviors and Applications of Silicon Oxides and Nitrides in Transient Electronics. *Adv. Funct. Mater.* **2014**, *24*, 4427−4434.

(11) Hwang, S.-W.; Park, G.; Edwards, C.; Corbin, E. A.; Kang, S.-K.; Cheng, H.; Song, J.-K.; Kim, J.-H.; Yu, S.; Ng, J.; Lee, J. E.; Kim, J.; Yee, C.; Bhaduri, B.; Su, Y.; Omennetto, F. G.; Huang, Y.; Bashir, R.;

Goddard, L.; Popescu, G.; Lee, K.-M.; Rogers, J. A. Dissolution Chemistry and Biocompatibility of Single-Crystalline Silicon Nanomembranes and Associated Materials for Transient Electronics. *ACS Nano* **2014**, *8*, 5843−5851.

(12) Hwang, S.-W.; Song, J.-K.; Huang, X.; Cheng, H.; Kang, S.-K.; Kim, B. H.; Kim, J.-H.; Yu, S.; Huang, Y.; Rogers, J. A. High-Performance Biodegradable/Transient Electronics on Biodegradable Polymers. *Adv. Mater.* **2014**, *26*, 3905−3911.

(13) Hwang, S.-W.; Kim, D.-H.; Tao, H.; Kim, T.-I.; Kim, S.; Yu, K. J.; Panilaitis, B.; Jeong, J.-W.; Song, J.-K.; Omenetto, F. G.; Rogers, J. A. Materials and Fabrication Processes for Transient and Bioresorbable High-Performance Electronics. *Adv. Funct. Mater.* **2013**, *23*, 4087−4093.

(14) Hwang, S.-W.; Huang, X.; Seo, J.-H.; Song, J.-K.; Kim, S.; Hage-Ali, S.; Chung, H.-J.; Tao, H.; Omenetto, F. G.; Ma, Z.; Rogers, J. A. Materials for Bioresorbable Radio Frequency Electronics. *Adv. Mater.* **2013**, *25*, 3526−3531.

(15) Jin, S. H.; Shin, J.; Cho, I.-T.; Han, S. Y.; Lee, D. J.; Lee, C. H.; Lee, J.-H.; Rogers, J. A. Solution-Processed Single-Walled Carbon Nanotube Field Effect Transistors and Bootstrapped Inverters for Disintegratable, Transient Electronics. *Appl. Phys. Lett.* **2014**, *105*, 013506-1−013506-4.

(16) Wu, X. S.; Wang, N. Synthesis, Characterization, Biodegradation, and Drug Delivery Application of Biodegradable Lactic/Glycolic Acid Polymers. Part II: Biodegradation. *J. Biomater. Sci., Polym. Ed.* **2001**, *12*, 21−34.

(17) Ponnusamy, T.; Lawson, L. B.; Freytag, L. C.; Blake, D. A.; Ayyala, R. S.; John, V. T. In Vitro Degradation and Release Characteristics of Spin Coated Thin Films of PLGA with a "Breath Figure" Morphology. *Biomatter* **2012**, *2*, 77−86.

(18) Makadia, H. K.; Siegel, S. J. Poly Lactic-*co*-Glycolic Acid (PLGA) as Biodegradable Controlled Drug Delivery Carrier. *Polymers* **2011**, *3*, 1377−1397.

(19) Sabir, M. I.; Xu, X.; Li, L. A Review on Biodegradable Polymeric Materials for Bone Tissue Engineering Applications. *J. Mater. Sci.* **2009**, *44*, 5713−5724.

(20) Lam, C. X. F.; Savalani, M. M.; Teoh, S.-H.; Hutmacher, D. W. Dynamics of in Vitro Polymer Degradation of Polycaprolactone-Based Scaffolds: Accelerated Versus Simulated Physiological Conditions. *Biomed. Mater.* **2008**, *3*, 034108-1−034108-15.

(21) Woodruff, M. A.; Hutmacher, D. W. The Return of a Forgotten Polymer—Polycaprolactone in the 21st Century. *Prog. Polym. Sci.* **2010**, *35*, 1217−1256.

(22) Hutmacher, D. W. Scaffold Design and Fabrication Technologies for Engineering Tissues — State of the Art and Future Perspectives. *J. Biomater. Sci., Polym. Ed.* **2001**, *12*, 107−124.

(23) Irimia-Vladu, M. "Green" Electronics: Biodegradable and Biocompatible Materials and Devices for Sustainable Future. *Chem. Soc. Rev.* **2013**, *43*, 588−610.

(24) Irimia-Vladu, M.; Troshin, P. A.; Reisinger, M.; Shmygleva, L.; Kanbur, Y.; Schwabegger, G.; Bodea, M.; Schwödiauer, R.; Mumyatov, A.; Fergus, J. W.; Razumov, V. F.; Sitter, H.; Sariciftci, N. S.; Bauer, S. Biocompatible and Biodegradable Materials for Organic Field-Effect Transistors. *Adv. Funct. Mater.* **2010**, *20*, 4069−4076.

(25) Bettinger, C. J.; Bao, Z. Organic Thin-Film Transistors Fabricated on Resorbable Biomaterial Substrates. *Adv. Mater.* **2010**, *22*, 651−655.

(26) Chiu, C. J.; Weng, W. Y.; Chang, S. J.; Chang, S.-P.; Chang, T. H. A Deep UV Sensitive Ta_2O_5/a-IGZO TFT. *IEEE Sens. J.* **2011**, *11*, 2902−2905.

(27) Yang, D. J.; Whitfield, G. C.; Cho, N. G.; Cho, P.-S.; Kim, I.-D.; Saltsburg, H. M.; Tuller, H. L. Amorphous $InGaZnO_4$ Films: Gas Sensor Response and Stability. *Sens. Actuators, B* **2012**, *171*, 1166−1171.

(28) Horasawa, N.; Nakajima, H.; Takahashi, S.; Okabe, T. Behavior of Pure Gallium in Water and Various Saline Solutions. *Dent. Mater. J.* **1997**, *16*, 200−208.

(29) Wataha, J. C.; Nakajima, H.; Hanks, C. T.; Okabe, T. Correlation of Cytotoxicity with Elemental Release from Mercury-

and Gallium-Based Dental Alloys in Vitro. *Dent. Mater.* **1994**, *10*, 298−303.

(30) Baddinga, M. A.; Stefaniakb, A. B.; Fix, N. R.; Cummings, K. J.; Leonard, S. S. Cytotoxicity and Characterization of Particles Collected from an Indium−Tin Oxide Production Facility. *J. Toxicol. Environ. Health, Part A* **2014**, *77*, 1193−1209.

(31) Yan, D.; Yin, G.; Huang, Z.; Liao, X.; Kang, Y.; Yao, Y.; Hao, B.; Gu, J.; Han, D. Biomineralization of Uniform Gallium Oxide Rods with Cellular Compatibility. *Inorg. Chem.* **2009**, *48*, 6471−6479.

(32) Webb, D. R.; Wilson, S. E.; Carter, D. E. Comparative Pulmonary Toxicity of Gallium Arsenide, Gallium(lll) Oxide, or Arsenic (lll) Oxide lntratracheally Instilled into Rats. *Toxicol. Appl. Pharmacol.* **1986**, *82*, 405−416.

(33) Li, Z.; Yang, R.; Yu, M.; Bai, F.; Li, C.; Wang, Z. L. Cellular Level Biocompatibility and Biosafety of ZnO Nanowires. *J. Phys. Chem. C* **2008**, *112*, 20114−20117.

(34) Lee, C. H.; Kim, D. R.; Zheng, X. Fabrication of Nanowire Electronics on Nonconventional Substrates by Water-Assisted Transfer Printing Method. *Nano Lett.* **2011**, *11*, 3435−3439.

(35) DeMerlis, C. C.; Schonker, D. R. Review of the Oral Toxicity of Polyvinyl Alcohol (PVA). *Food Chem. Toxicol.* **2003**, *41*, 319−326.

(36) Paradossi, G.; Cavalieri, F.; Chiessi, E. Poly(vinyl alcohol) as Versatile Biomaterial for Potential Biomedical Application. *J. Mater. Sci.* **2003**, *14*, 687−691.

(37) Sedra, A. S.; Smith, K. C. *Microelectronic Circuits*, 6th ed.; Oxford University Press, Inc.: New York, 2010; Chapter 13, p 1075.

(38) Kang, S.-M.; Leblebici, Y. *CMOS Digital Integrated Circuits: Analysis and Design*; McGraw-Hill Companies Inc.: New York, 1996; Chapter 6, p 216.

(39) Brumbach, M.; Armstrong, N. R. *Encyclopedia of Electrochemistry*; Wiley-VCH: Weinheim, 2007; Chapter 1.1.2, p 18; DOI: 10.1002/9783527610426.bard100101.

(40) Baric, A.; Branica, M. Behavior of Indium in Seawater. *Limnol. Oceanogr.* **1969**, *14*, 796−798.

(41) Krebs, H. A. Chemical Composition of Blood Plasma and Serum. *Annu. Rev. Biochem.* **1950**, *19*, 409−430.

(42) Chen, Y.; Wu, J.; Dong, C.; Shi, J.; Zhan, R. Development of Source/Drain Electrodes for Amorphous Indium Gallium Zinc Oxide Thin Film Transistors. *Dig. Tech. Pap. - Soc. Inf. Disp. Int. Symp.* **2013**, *46.3*, 640−643.